

Dipole blockade through Rydberg Förster resonance energy transfer

Thibault Vogt,^{*} Matthieu Viteau, Jianming Zhao,[†] Amodsen Chotia, Daniel Comparat, and Pierre Pillet
Laboratoire Aimé Cotton,[‡] CNRS, Bât. 505, Campus d'Orsay, 91405 Orsay, France

(Dated: 15 February 2006)

High resolution laser excitation of np Rydberg states of cesium atoms shows a dipole blockade at Förster resonances corresponding to the resonant dipole-dipole energy transfer of the $np + np \longrightarrow ns + (n+1)s$ reaction. The dipole-dipole interaction can be tuned on and off by the Stark effect, and such a process observed for relatively low n ($25 - 41$) is promising for quantum gate devices. Both Penning ionization and saturation in the laser excitation can limit the range of observation of the dipole blockade.

PACS numbers: 32.80.Rm; 32.80.Pj; 34.20.Cf; 34.60.+z

Rydberg atoms have long been known to possess huge electric dipole moments leading to exaggerated collisional properties of room temperature atoms, in particular, large cross sections and long interaction times [1]. These properties have stimulated great interest in the possibility of controlling the strong long-range interactions between cold atoms [2, 3, 4], which could be particularly exciting for quantum information applications [5, 6]. One interesting process is the possibility of dipole blockade in the Rydberg excitation of atoms, due to the dipole-dipole interaction shifting the Rydberg energy from its isolated atomic value. If the volume of the laser excitation is small enough, no second atom can be excited after the Rydberg excitation of the first one, producing an atomic ensemble in a singly excited collective state. The use of the dipole blockade of the excitation has been proposed as a very efficient realization of a scalable quantum logic gate [6]. If we consider the laser high-resolution-excitation of a large ensemble of atoms from the ground state or from a low-excited state towards a Rydberg state, the dipole-dipole interaction between Rydberg atoms should lead to a limitation of the number of excited atoms versus the initial density of atoms. A partial, or local, blockade of the excitation is thus expected. The first excited Rydberg atoms shift the resonance for their non-excited neighbors and prevent their excitation with a narrow-bandwidth laser.

Up to now no evidence of a dipole blockade has been demonstrated. In zero electric field, the atomic Rydberg state do not have permanent dipole moments and no dipole blockade is expected. Second order dipole-dipole or van der Waals coupling between Rydberg atoms can occur, and a suppression of the excitation corresponding to a partial, or local, blockade has been reported in excitation of high Rydberg states ($n \sim 70 - 80$) using a pulse amplified single mode laser [7]. Cw excitations have

also been performed showing the suppression of the excitation [8] and studying the sub-Poissonian atom counting statistics [9]. The authors notice that for long-duration excitations, appearance of ions can lift the blockade. For a broad-band excitation, the suppression of the excitation is not expected. Rather a band of levels can be excited with a density-dependent broadening, which has been probed using micro-wave transitions [10], or laser depumping [11]. In high electric field, the Stark effect mixes the Rydberg states, and the Rydberg atoms have a significant permanent dipole moment. The dipole blockade is expected but the presence of both dipole-dipole and van der Waals couplings complicate the evolution of the blockade versus the electric field. An alternative is the use of a configuration of strong dipole-dipole coupling in low electric field with relatively low Rydberg states, similar to Förster resonances [12]. The Förster (or Fluorescence) Resonance Energy Transfer (FRET) is commonly used as spectroscopic technique based on long-range dipole-dipole coupling to estimate small distance and dynamics between fluorescent molecules [13, 14].

In this letter, we report the observation of the dipole blockade of the Rydberg excitation by cw lasers, by taking advantage of a resonant dipole-dipole coupling of cesium atoms, specifically the process

$$np_{3/2} + np_{3/2} \longrightarrow ns + (n+1)s. \quad (1)$$

The dipole-dipole interaction is $W \sim \mu\mu'R^{-3}$, where μ , $\mu' \sim n^2$ atomic units are the dipoles corresponding to the transitions $np_{3/2} \longrightarrow ns$ and $np_{3/2} \longrightarrow (n+1)s$, respectively, and R the distance between the two atoms. Control of the dipole-dipole coupling is achieved by using the Stark effect. The resonance is obtained when, by Stark shifting, the level $np_{3/2}$ is located midway in the energy diagram between the states, ns and $(n+1)s$ [2]. At such resonances, also called Förster resonances, we observe a significant decrease of the p excitation, interpreted as a local dipole blockade.

The details of the experimental setup have been described in several papers [2, 4, 11]. But here, three cw lasers provide a new high resolution multistep scheme of excitation, as depicted in Fig.1 (a). The Rydberg atoms

[†]Visitor from College of Physics and Electronics Engineering, Shanxi University, China.

[‡]Laboratoire Aimé Cotton is associated to Université Paris-Sud and belongs to Fédération de Recherche Lumière Matière (LUMAT).

^{*}Electronic address: thibault.vogt@lac.u-psud.fr

are excited from a cloud of $5 \cdot 10^7$ cesium atoms (temperature $200 \mu\text{K}$, characteristic radius $\sim 300 \mu\text{m}$, peak and average density $2 \cdot 10^{11}$ and $4 \cdot 10^{10} \text{ cm}^{-3}$, respectively) produced in a standard vapor-loaded magneto-optical trap (MOT) at residual gas pressure of 10^{-10} mbar . The first step of the excitation, $6sF = 4 \rightarrow 6p_{3/2}F = 5$, is provided by the trapping lasers of the MOT. The density of excited, $6p_{3/2}$, atoms present in the MOT can be modified by switching off the repumper lasers of the MOT, with a delay ranging from 0 to 1 ms before applying the other steps of the excitation. We use an infrared diode laser (DL100 TOPTICA) with a wavelength of $\lambda_2 = 1.47 \mu\text{m}$ in an extended cavity device for the second step of the excitation, $6p_{3/2}F = 5 \rightarrow 7sF = 4$. The bandwidth is of the order of 100 kHz and the available power is 20 mW. The last step of the excitation, $7sF = 4 \rightarrow np_{3/2}$ (with $n = 25 - 45$), is provided by a Titanium:Sapphire (Ti:Sa) laser pumped by an Ar^+ laser. The wavelength λ_3 ranges from 770 to 800 nm, the bandwidth is 1 MHz, and the available power is 400 mW. The Ti:Sa laser is switched on during a time, $\tau = 0.3 \mu\text{s}$ by means of an acousto-optic modulator. The beams of the infrared diode laser and of the Ti:Sa laser cross with an angle of 67.5 degrees and are focused into the atomic cloud with waists of 105 and $75 \mu\text{m}$ respectively. Their polarizations are both linear and parallel to the direction of the applied electric field, leading to the excitation of the magnetic sublevel $|m| = 1/2$ for $np_{3/2}$. The spectral resolution, $\Delta\nu$, of the excitation is of the order of $5 - 6 \text{ MHz}$, limited by the lifetime, 56.5 ns , of the $7s$ state and by the duration and the spectral width of the Ti:Sa laser pulse. The magnetic quadrupole field of the MOT is not switched off during the Rydberg excitation phase, it contributes for less than 1 MHz to the observed linewidths. The average intensity ($\sim 3 \text{ mW/cm}^2$) of the infrared diode laser is chosen to reach saturation of the transition ($\sim 1.4 \text{ mW/cm}^2$). At the trap position, a static electric field and a pulsed high voltage field are applied by means of a pair of electric field grids spaced by 15.7 mm. We analyze selectively the Rydberg states by applying just after the Ti:Sa laser pulse a field ramp with a rise time of 700 ns, and by detecting the ions with a pair of microchannel plates.

The experimental procedure consists of Stark spectroscopy of the $np_{3/2}$ states at a repetition rate of 80 Hz for different atomic densities, and for different Ti:Sa laser intensities. During the excitation process a small number, ~ 100 , of ions less than one percent of the total number of Rydberg atoms is formed, which we attribute to cold collisions between Rydberg atoms [15]. These ions are simultaneously detected with the Rydberg atoms. Fig.2 shows the analysis of spectra of the $38p_{3/2}$ state performed at different values of the electric field. At zero electric field, the number of excited Rydberg atoms is about 11 000, corresponding to an estimated average density of $2 \cdot 10^9 \text{ cm}^{-3}$. The electric field dependence of the width, the total number of atoms excited, and the num-

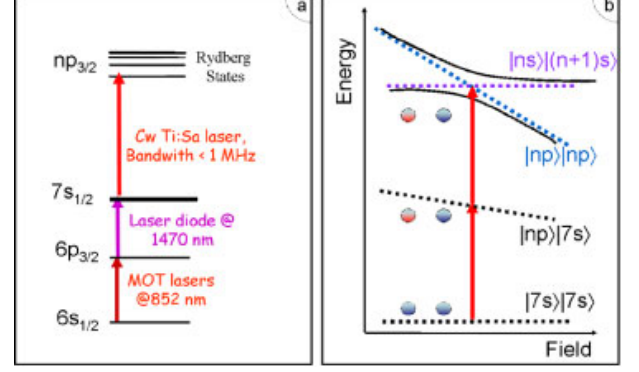


FIG. 1: (Color online) Representations (a) of the three-step scheme of excitation for $np_{3/2}$ Rydberg states, and (b) of the excitation of a pair of atom at the Förster resonance. The dipole-dipole coupling leads to an avoiding crossing between the energy levels $|np_{3/2}\rangle \otimes |np_{3/2}\rangle$ and $|ns\rangle \otimes |(n+1)s\rangle$ of the pair of atoms.

ber of ions present in the Rydberg sample at the end of the excitation are shown in Figs.2 (a, b, c). First we observe a minimum in the number of excited atoms at the resonance of the reaction of Eq. (1), at $F = 1.46 \text{ V/cm}$. The width of the lines away from the Förster resonance is 6 MHz, the limit of resolution of the multistep laser excitation. It is increased at the resonance to 8 – 9 MHz. At the resonance, we do not observe any increase in the number of ions. In the high field wing of the resonance, we can observe a small increase of this number, up to 200, which corresponds to a Penning ionization process by exciting pairs of close atoms which are subjected to an attractive force [11, 15]. The number of ions stays small enough to add no broadening to the line. Figs.2 (d, e) show the selective detection of the population in the $38p_{3/2}$ state and the population transferred in the $38s$ state versus the electric field. The resonance in the s signal is at the same position as the minimum of the p excitation, both curves presenting the same width versus the electric field.

Fig.3 shows the evolution of the amplitudes of the $np_{3/2}$ excitation versus the electric field for different principal quantum numbers $n = 42, 40, 38, 36$, and 25. Except for $n = 42$, we observe a minimum corresponding to the resonance of the reaction of Eq. (1). For $n \geq 42$, the energy of a pair of atoms $np_{3/2} + np_{3/2}$ becomes smaller than the one of a pair $ns + (n+1)s$, and the Förster resonance no longer exists. Nevertheless at $n = 42$, the difference between the energy levels of a pair of atoms is only -9.5 MHz , small enough to observe a decrease of the excitation at zero field. The data show a clear dipole blockade of the excitation of up to 30% for $n = 40, 38$, and 36. For each n , we observe also a small increase in the width of the spectral line of the $p_{3/2}$ excitation at the Förster resonance. For lower n , ~ 25 , a less important

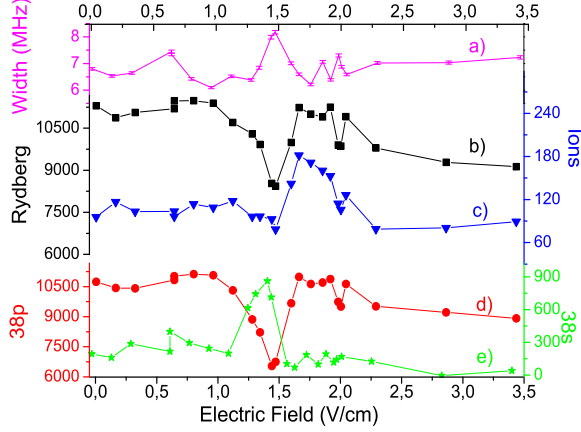


FIG. 2: (Color online) Detailed study of the dipole blockade for the $38p_{3/2}$ state. The Ti:Sa laser is resonant with the transition $7s \rightarrow 38p_{3/2}$ and its power is kept constant at 8 mW corresponding to an average intensity of 45 W/cm^2 . Versus the applied electric field: (a) linewidths, (b) total number of Rydberg atoms, (c) number of ions, (d) and (e) number of atoms in $38p_{3/2}$ and $38s$, respectively.

dipole blockade of the excitation is also observed but no real broadening of the spectral lines.

One property of the dipole blockade of the excitation is that it should be dependent on the atomic density and on the laser excitation. Fig.4 shows the evolution of the dipole blockade in the case of the $36p_{3/2}$ state. We have plotted the number of excited Rydberg atoms, $36p_{3/2}$, at the Förster resonance versus the one out of resonance obtained for two different average atomic densities corresponding for the $7s$ state, respectively $\sim 8 \pm 3 \cdot 10^9$ (which

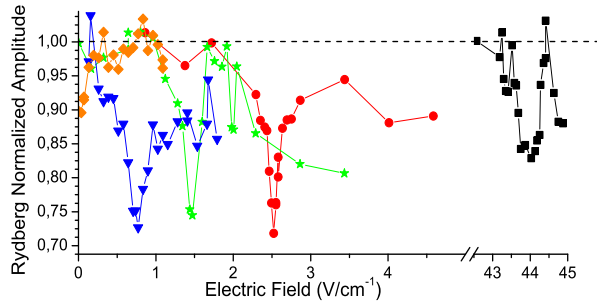


FIG. 3: (Color online) Normalized number of excited Rydberg atoms, for the same experimental conditions as in Fig.2, versus the applied electric field for different $np_{3/2}$ states: $42p_{3/2}$ (diamonds symbols), $40p_{3/2}$ (triangles), $38p_{3/2}$ (stars), $36p_{3/2}$ (circles), and $25p_{3/2}$ (squares). The Förster resonances occur at fields of 0.75, 1.46, 2.53, and 44.03 V/cm. The normalisation is performed by considering the maximum field amplitude, except $n = 25$, for which the signal at 43.17 V/cm is normalized to one.

is used for most of reported results) and $2.7 \cdot 10^9 \text{ cm}^{-3}$. First we see the appearance of the dipole blockade when the number of Rydberg atoms exceeds 1000. Both curves present then the same blockade up to a Rydberg excitation of 3500 atoms. Above this point, the evolution of both curves differs. When the number of Rydberg atoms exceeds 5000, the effect of dipole blockade disappears in the case of an initial $7s$ state density of $2.7 \cdot 10^9 \text{ cm}^{-3}$, while its efficiency goes on to increase for a three times larger density. This result can seem quite surprising and is linked to the saturation of the excitation. Experimentally, the number of Rydberg atom varies linearly with the power of the Ti:Sa laser up to 4 mW, corresponding to an intensity of 22 W/cm^2 , then the excitation starts to saturate. For instance on Fig.4, to obtain 5000 Rydberg atoms, we need five times more power (6 and 30 mW, respectively) while the atomic density of $7s$ state is only three times smaller. We observe a broadening of the resonance with the laser power (see Fig.4 (a)) independent on the atomic density. By increasing the laser power from 0.1 to 10 mW we observe an increase in the efficiency of the dipole blockade. If we increase more the power of the Ti:Sa laser the dipole blockade becomes less efficient. Indeed, at high laser power the resonance lines are broadened, such that the laser excitation of pairs of closer atoms become possible, preventing the dipole blockade. The range in density and laser intensity allowing observation of the dipole blockade is therefore limited, and the dipole blockade results shown in Figs.2 and 3 correspond to the optimum of our experimental conditions, with a low power of the Ti:Sa laser (linewidth $\sim \Delta\nu$) and a high atomic density. At this point of this letter, we understand most of the features of the experiment, the observed dipole blockade seems to indicate that at the Förster resonance no pair of close atoms can be excited at a distance smaller than $R_{\min} \sim (\mu\mu'/W)^{1/3} \sim (\mu\mu'/\Delta\nu)^{1/3}$, which corresponds for $n = 38$ to $\sim 4 \text{ }\mu\text{m}$, in agreement with the measured Rydberg atom number and average Rydberg density, 8500 and $1.7 \cdot 10^9 \text{ cm}^{-3}$ ($W \sim 2.5 \text{ MHz}$ by considering the average density and 5.5 MHz for the peak one).

An unexpected result is that the width of the Förster resonance versus the static electric field (see Fig.1 (b)), which converted to frequency ($50 \pm 10 \text{ MHz}$ in the case of Fig.2 (b)) is much larger than the width of the spectral line (8 MHz shown in the inset of Fig.4 (b)). The resolution of this paradox lies probably in the dynamics of the dipole-dipole coupling during the Rydberg excitation, where many-body interactions are not negligible. The many-body effects are linked to the migration of the s state (ns or $(n+1)s$) excitation in the p state environment by excitation exchange due to dipole-dipole coupling in the frozen Rydberg gas, *i.e.* by the resonant processes:

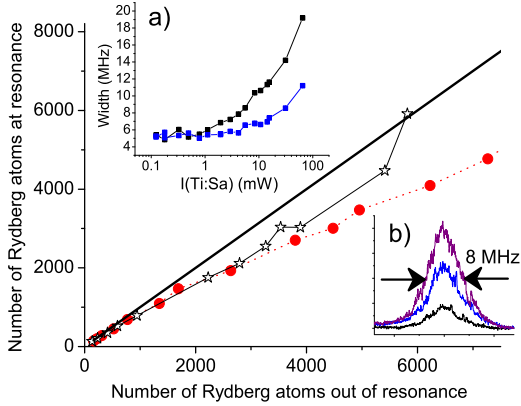


FIG. 4: (Color online) Number of $36p_{3/2}$ Rydberg atoms excited at the Förster resonance (2.53 V/cm) versus the one out of resonance (1.37 V/cm), for two different initial atomic densities of $7s$ state, $8 \cdot 10^9$ (filled circles) and $2.7 \cdot 10^9$ (empty stars). The efficiency of the blockade is the gap to the full (with a slope of 1) and broken lines. (a) Linewidths of laser resonance ($7s \rightarrow 36p_{3/2}$) at two electric field values: 2.52 (Förster resonance: upper curve), 1.37 (lower curve) V/cm. (b) Resonances for 0.8, 3.0 and 4.2 mW laser power. The broadening varies from 6 to 8 MHz as the laser power.

$$\begin{aligned}
 ns + np_{3/2} &\rightarrow np_{3/2} + ns, \\
 \text{and } (n+1)s + np_{3/2} &\rightarrow np_{3/2} + (n+1)s. \quad (2)
 \end{aligned}$$

The R^{-3} character of the dipole-dipole interaction makes the dipole blockade mostly result of two-body effects, meaning during the excitation each atom is essentially sensitive to its closest Rydberg neighbor. Nevertheless, in the local blockade process a pair of atoms at distance of the order of R_{\min} can be excited and interact with the energy transfer of Eq. (1) and the many-body effects of Eq. (2) occur. The role of the migration of the s state excitation is to increase the number of s Rydberg atoms in the sample, because a pair of close Rydberg, p , atoms can react several times [2]. Such an ensemble of s excitation enhances probably the blockade outside Förster resonance, where the $sp \rightarrow ps$ dipole-dipole interaction is always resonant, while the reaction of Eq.(1) is no longer resonant and less efficient. The broad band of the Förster resonance is a signature for the many-body behavior, while the narrow laser resonances are ones for two-body interaction.

To conclude, we have shown clear evidence for a local dipole blockade of the Rydberg excitation at a Förster resonance, controlled via the Stark effect. This result is not only promising for quantum information but offers a lot of applications. The use of a second laser scanned around the transition $7s \rightarrow np_{3/2}$ should permit us to excite pairs of very close atoms with a repulsive or an attractive mutual force. The band of levels due to the

Rydberg interactions can also be probed by microwave excitation [10, 18]. The precise shape of the resonance should be an excellent probe of the random character of the distribution of the pairs [19]. The Stark control of the dipole blockade should also allow us to prepare Rydberg atomic samples with pairs of repulsive or attractive atoms to analyze the formation of ions and the evolution towards an ultracold plasma [20, 21]. The observation of the total dipole blockade, meaning the excitation of a single atom, is still a challenge. It implies a volume of the Rydberg sample with a radius of the order of R_{\min} . Here we observe the Förster resonance up to $n = 41$, limiting R_{\min} at the value of $4 \mu\text{m}$. The choice of another Förster configuration with n of the order of 100 or more increases R_{\min} up to $20 \mu\text{m}$. A microwave field instead of the Stark effect could also be used to produce the dipole moments and to control the dipole blockade [22, 23].

This work is in the frame of "Institut francilien de recherche sur les atomes froids" (IFRAF) and of the European Research and Training Networks COLMOL (HPRN-CT-2002-00290) and QUACS (HPRN-CT-2002-00309). One of the authors (J. Z.) is supported by IFRAF. The cw excitation development corresponds to a preliminary study for the CORYMOL experiment supported by an ANR grant (NT05-2 41884). The authors acknowledge very fruitful discussions with Thomas F. Gallagher, Marcel Mudrich, Nassim Zahzam, and Vladimir Akulin.

-
- [1] T. F. Gallagher, *Rydberg Atoms* (Cambridge University Press, New York, 1994).
 - [2] I. Mourachko *et al.*, Phys. Rev. Lett. **80**, 253 (1998).
 - [3] W. R. Anderson *et al.*, Phys. Rev. Lett. **80**, 249 (1998).
 - [4] A. Fioretti *et al.*, Phys. Rev. Lett. **82**, 1839 (1999).
 - [5] D. Jaksch *et al.*, Phys. Rev. Lett. **85**, 2208 (2000).
 - [6] M. D. Lukin *et al.*, Phys. Rev. Lett. **87**, 037901 (2001).
 - [7] D. Tong *et al.*, Phys. Rev. Lett. **93**, 063001 (2004).
 - [8] K. Singer *et al.*, Phys. Rev. Lett. **93**, 163001 (2004).
 - [9] T. CubelLiebisch *et al.*, Phys. Rev. Lett. **95**, 253002 (2005).
 - [10] K. Afrousheh *et al.*, Phys. Rev. Lett. **93**, 233001 (2004).
 - [11] M. Mudrich *et al.*, Phys. Rev. Lett. **95**, 233002 (2005).
 - [12] T. F. Gallagher *et al.*, Phys. Rev. A **25**, 1905 (1982).
 - [13] T. Förster, in *Modern Quantum Chemistry* (Academic Press, New York, 1996).
 - [14] T. Förster, Discuss. Faraday Soc. **27**, 7 (1959).
 - [15] W. Li, P. J. Tanner, and T. F. Gallagher, Phys. Rev. Lett. **94**, 173001 (2005).
 - [16] W. M. Akulin *et al.*, Physica D **131**, 125 (1999).
 - [17] J. S. Frasier *et al.*, Phys. Rev. A **59**, 4358 (1999).
 - [18] I. Mourachko *et al.*, Phys. Rev. A **70**, 031401(R) (2004).
 - [19] V. M. Akulin, *Coherent Dynamics of Complex Quantum Systems* (Springer, 2006).
 - [20] M. P. Robinson *et al.*, Phys. Rev. Lett. **85**, 4466 (2000).
 - [21] W. Li *et al.*, Phys. Rev. A **70**, 042713 (2004).
 - [22] P. Pillet *et al.*, Phys. Rev. A **36**, 1132 (1987).

- [23] P. Pillet *et al.*, in *Decoherence, Entanglement and Information Protection in Complex Quantum Systems* (pages 411-436), edited by V. M. Akulin *et al.*, vol. 189 (NATO Sciences Series II, 2005).